Science Journal of Analytical Chemistry
2025, Vol. 13, No. 4, pp. 84–95
https://doi.org/10.11648/j.sjac.20251304.12

Research Article

Quantum Chemical Study of Methyl Substituent's Position on Quinoline for Inhibition of Aluminium Corrosion inHydrochloric Acid Solution

Abdulmumin Malam Usman[1, *], Ayuba Abdullahi Muhammad[2], Jaweria Ambreen[3, 4], Jamilu Ahmad Bello[5], Najib Usman Shehu[2]

[1]DepartmentofAppliedChemistry, Federal University of Technology, Babura, Nigeria
[2]Department of Pure and Industrial Chemistry, Bayero University, Kano, Nigeria
[3]Department of Biomedical Engineering, University Teknologi Malaysia, Johor Bahru, Malaysia
[4]Department of Chemistry, COMSATS University, Islamabad, Pakistan
[5]Department of Chemistry, Northwest University Kano, Nigeria

Abstracts

Quantum chemical study of some methylquinolines on inhibition of aluminium corrosion in hydrochloric acid and effect of methyl group at 5, 7 and 8 position on quinoline was investigated theoretically with the aid of material studio using density functional theory (DFT). The simulations were performed by means of the DFT electronic program DMol^3 using the Mulliken population analysis in the Material Studio. DMol^3 permitted the analysis of the electronic structures and energies of molecules, solids and surfaces. The analysis of the quantum chemical parameters, the adsorption parameters form the simulation of the molecules, the Mulliken and Hirshfeld values of the fukui indices for the three molecules of the 5-MeQ, 7-MeQ and 8-MeQ indicated that all the three molecules exhibits high potential for inhibition of aluminium corrosion in HCl environment, with 5-MeQ being the best among all. The most popular parameters which play a prominent role are the eigen values of the highest occupied molecular orbital (HOMO) and lowest unoccupied molecular orbital (LUMO), the HOMO-LUMO gap (ΔE), chemical hardness and softness, electro-negativity and the number of electrons transferred from inhibitor molecule to the metal surface. All the molecules showed good corrosion inhibition tendency, however, 5-MeQ molecule gives better aluminium corrosion inhibition potential than other two molecules. The orientation of the Methyl substituent on the core quinoline was found to be responsible for intra-molecular intraction which leads to weaker attraction to the aluminium surface for the 7-MeQ and 8-MeQ molecules hence lower corrosion inhibition tendency than 5-MeQ molecule despite having the same molecular mass.

Keywords

Methylquinoline, Aluminium, Corrosion, Substituent, Position, Inhibition Quantum, Chemical Parameters

*Corresponding author: amusman.chemistry@futb.edu.ng (Abdulmumin Malam Usman)

Received: 27 June 2025; **Accepted:** 14 July 2025; **Published:** 24 December 2025

1. Introduction

Generally the study of corrosion inhibition activity by some organic molecules and their derivatives on metals has been the subjects of investigations in the quest to design a befitting inhibitor on the basis of properties and environment of the metal in question [1]. However, a wide range of organic inhibitors offers desirable attributes such as non-toxicity, a variety of choices and readily availability [2]. Meanwhile, they cannot universally protect all metals in the same aggressive media, thus prompting the search for efficient metal or medium-specific inhibitors. Consequently, organic inhibitors of various classes have been the subject of intensive research interest as potential materials for the surface protection of ferrous and non-ferrous metals and their alloys against aggressive environments [3].

Just like iron, aluminium is globally widespread in application, and as one of the less noble non-ferrous metal it has a strong tendency to undergo all forms of corrosion in aggressive environments. Despite having a protected oxides films, it do undergo passivation (gradual removal of the protective oxides). The extraction of aluminium from its ore (bauxite) is virtually energy extensive and economically expensive necessitating the needs for protection against severe corrosion attack in corrosive environment [4, 5].

Hydrochloric acid is a common acidic medium for these purposes because it is more economical, efficient and less troublesome compared to other mineral acids. In the actual facts, Cl^- from various sources including neutral salts, has the ability to cause pitting corrosion at vulnerable spots of passive film-protected non-ferrous metal [6].

Many experimental methods and modern surface characterization tools have been created to evaluate and characterize the performance of corrosion inhibitors for metals and alloys [7]. These methodologies are often expensive, time consuming and tedious. Computational methods have already proven to be very useful in determining the inhibitors molecular structure and elucidating its electronic properties and reactivity. The aim of assessing the efficiency of a corrosion inhibitor, with the help of computational chemistry tools, is to search for compounds with desired properties, using mathematically quantified and computerized forms [7]. The development of DFT, force fields and molecular dynamic (MD) simulations, abolition, semi-empirical and Hartree-Fock model approaches provides potential solutions [8]. The pioneering work of Hohenberg and Kohn (1964) and Kohn and Sham (1965) [8] has made DFT one of the more popular tools among computational chemical methods, because it focuses on the electron density P(r) as the carrier of all information in the molecular ground state, rather than on a single-electron wave function [9]. Several molecular parameters and descriptors widely used in the molecular characterization of corrosion inhibitors' effectiveness on the metal surfaces have been derived from DFT. Computational chemistry serve as a modern tool in developing novel molecules for the protection of metals and alloys that are important engineering contributors [10].

Methylquinolines are nitrogenous bicyclic heterocyclic compound with molecular formula of C_9H_9N, as such it is expected to show a reasonable inhibition against metallic corrosion because of its association with high electron density (10-π and 2-nonbondinggvc electrons) [11, 12]. Quinoline derivatives containing polar substituent such as methyl ($–CH_3$) can effectively adsorb and form highly stable chelating complexes with surface metallic atoms through coordination bonding [8]. The available studies for corrosion inhibition of quinoline molecules focuses on the nature and type of functional groups (being substituted or non-substituted) attached to the quinoline molecule. To our knowledge, this is the first investigation for effect of position of substituent groups in corrosion inhibition for aluminium in acidic environment by quantum chemical method. However, the following Figures 1, 2 and 3 are the structures of the methyl substituted quinolines at position five, seven and eight respectively as investigated by computational method.

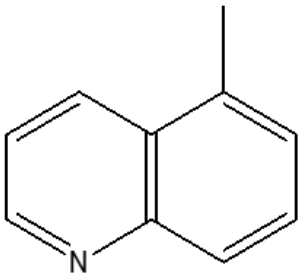

5-methylquinoline

Figure 1. *The structure of 5-MeQ.*

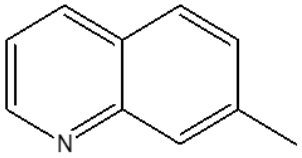

7-methylquinoline

Figure 2. *The structure of 7-MeQ.*

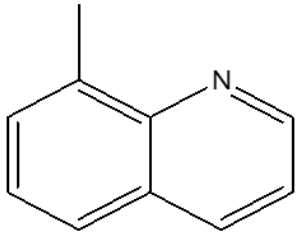

8-methylquinoline

Figure 3. *The structure of 8-MeQ.*

2. Methodology

2.1. Materials

The materials and instruments used in this research include: aluminium, hydroxy-quinoline derivatives and Dell Computer Core i5 16G RAM of high resolution, install with Material studio Version 2017.

2.2. Procedures

2.2.1. Sketching of Molecules

Materials Studio icon on the desktop was double-click to start the program. New project dialogue was opened and named according to structure of interest (5-MeQ, 7-MeQ, or 8-MeQ,). This starts by sketching a ring, followed by the remaining parts of the molecule to produce the substituted quinoline molecule. This was achieved by choosing *File*, followed by *New*, from the menu bar to open the *New Document* dialogue.*3D Atomistic*was selected from the options and the *Ok* button was clicked.To sketch a ring and/or cyclic compounds, four, five and six membered rings are provided as templates in Materials Studio and can be sketched easily using the Sketch Ring tool. The *Sketch Ring* button was clicked on the Sketch toolbar. The cursor changed to the sketching cursor, with a number 6 in the centre of a ring denoting that a six-membered ring was drawn when clicking in the new document. The next step was to place the phenyl ring in the *3D Atomistic document*. By default, the Sketch Ring tool generates a ring of carbons connected by single bonds. So, for a six-membered ring, it typically produces a cyclohexane ring minus the hydrogen atoms. However, by holding down the *ALT key and clicking in the 3D Viewer*, an aromatic ring was added directly. Other part of the molecule were attached to the ring by selecting the element in the dropdown list under '*Element used to sketch*" arrow. The cursor was moved over one of the carbon atoms in the 3D Viewer. When the atom changed colour to light blue, it was clicked on it. The cursor was moved away to sprout a bond. It was clicked again to place the other atoms eg carbon atom. Substituents are attached to appropriate position to create the quinoline derivative (eg 5-methylquinoline etc). The *ESC* key was pressed to cancel further drawing (Materials Studio 8, 2017).

The change in colour of the carbon atom as the cursor moves over it indicates that the carbon can be selected. After attaching all the required atoms to the molecule, the final step was to add the hydrogen atoms by clicking the *Adjust Hydrogen* button on the toolbar. The Adjust Hydrogen tool automatically fills up any empty valences in a structure with hydrogen atoms to satisfy them. The sketched structure needs to be cleaned by using the *Clean* tool to tidy up the geometry.

2.2.2. Optimization of the Molecules

The sketched molecules will not have an accurate geometry, so all molecules were subjected to geometry optimization to refine the geometry of their structures so as to minimize their torsional and conformational energies as well as global minimum energy of the molecules. This was achieved using the $DMol^3$ geometry optimization task in Accelrys Material Studio 8.0. The access to the $DMol^3$ optimization dialog box which allows the set up and displays the parameters that control the simulation in a $DMol^3$ optimization dialog task was traced either through the menu or through the Modules toolbar. The $DMol^3$ toolbar on the Modules toolbar was clicked and Calculation from the dropdown list/task bar was selected to display the $DMol^3$ calculation dialog box where the following properties; task: geometry optimization, quality: fine were selected, which set the geometry optimization convergence thresholds for any change, maximum force and minimum displacement between optimization cycles. The optimization stopped when the energy convergence was satisfied, along with either the displacement or gradient criteria. If the calculated initial gradients were below the threshold, the optimization will successfully stop without making a single step and without comparing displacements and energies. Three sets of convergence thresholds were available; coarse, medium and fine. The fine was selected which have values of 1×10^{-5} energy (Hartree), maximum force (Hartree $Å^{-1}$) of 0.002 and maximum displacement (Å) of 0.05. The use symmetry box was checked, indicating that the symmetry information was used in the calculation, while spin unrestricted box which searches for spin unrestricted solution was not checked. The exchange correlation functional theory level, LDA was selected followed by the PWC local density functional to be used was also selected. The geometry optimization was conducted and the optimized structures were saved for further use in quantum calculations of some structural and electronic properties. The following are the parameters to be assessed:

HOMO (at orbital number), LUMO (at orbital number), Molecular Mass (g/mol), Dipole Moment (Debye), E_{HOMO} (eV), E_{LUMO} (eV), Gap Energy (ΔE) (eV), Ionization Potential (IP) (eV), Electron Affinity (EA) (eV), Global Hardness (η) (eV), Global Softness (σ) $(eV)^{-1}$, Absolute Electronegativity (χ) (eV), Chemical Potential (μ) (eV), Global Electrophilicity Index (ω) (eV), Nucleophilicity Index (ε) $(eV)^{-1}$, Electron Donating Power (ω^-) (eV), Electron Accepting Power (ω^+) (eV), Net Electrophilicity ($\Delta\omega^{\pm}$) (eV), Energy of Back Donation ($\Delta E_{b\text{-}d}$) (eV), Total Number of Electrons, Fraction of Electrons Transferred (ΔN) [13-15].

2.2.3. Calculation of the Quantum Chemical Parameters

The electronic structure of the molecules, including the distribution of frontier molecular orbitals E_{HOMO} and E_{LUMO}, Fukui indices were assessed, with a view to establishing the active

sites as well as local reactivity of the molecule [16]. The simulations were performed by means of the Density Functional Theory (DFT) electronic program DMol^3 using the Mulliken population analysis in the Material Studio 8.0 software. DMol^{3}permits analysis of the electronic structures and energies of molecules, solids and surfaces using DFT. Electronic parameters for the simulations include restricted spin polarization using the DND basis set and the Perdew Wang local correlation density functional. Local reactivity of the studied compounds was analysed by means of the Fukui indices (FI) to assess regions of nucleophilic and electrophilic behaviour. The electronic and structural properties of a sketched molecule was requested through the Properties tab of the DMol^3 calculation dialog. These properties were computed as part of the calculation and viewed using the DMol^3 Analysis dialog. The properties that can be accessed through the Properties tab include: band structure, density of states (DOS), electron densities, frequencies, Fukui functions, optics, orbitals and population analysis (Materials Studio 8, 2017).

2.2.4. Quench Molecular Dynamic Simulation

One common molecular dynamics method, called quench molecular dynamics, perform a standard molecular dynamics calculation with an additional geometry optimization step, in which a geometry optimization is performed on every frame in the trajectory file. Effectively, molecular dynamics is used to sample many different low energy configurations (Materials Studio 8, 2017).

In this work, Forcite Plus were used to perform molecular dynamics on a system comprising organic molecules (The quinoline derivatives), and a metal (aluminium) surface. The aluminium surface was cleaved from the rutile form of the aluminium crystal structure. The molecule was placed on the surface, optimized before quench molecular dynamics was ran. A study table was used to look for the lowest energy conformation and finally was also used to calculate the binding energy which is the ultimate target (Materials Studio 8, 2017).

3. Results and Discussions

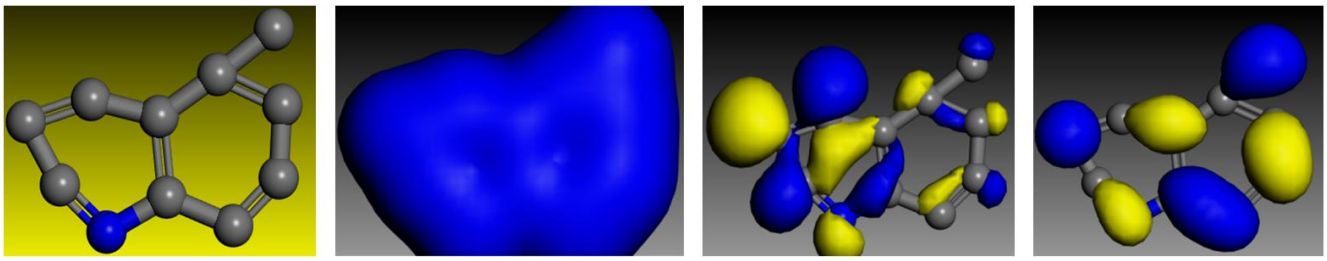

Figure 4. *Optimized structure, electrondensity, HOMO and LUMO of 5-MeQ.*

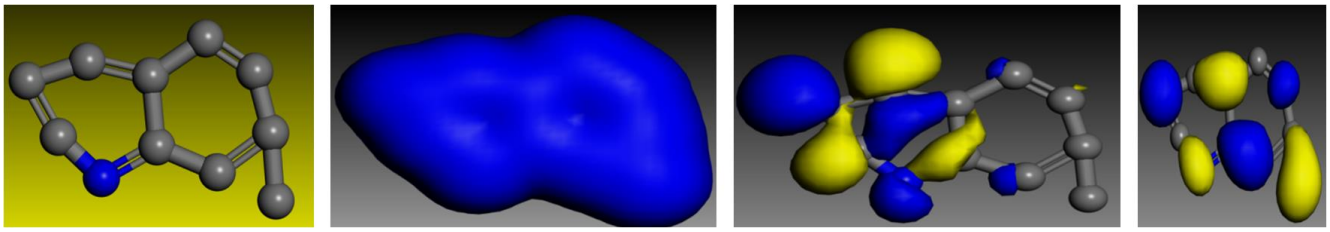

Figure 5. *Optimized structure, electrondensity, HOMO and LUMO of 7-MeQ.*

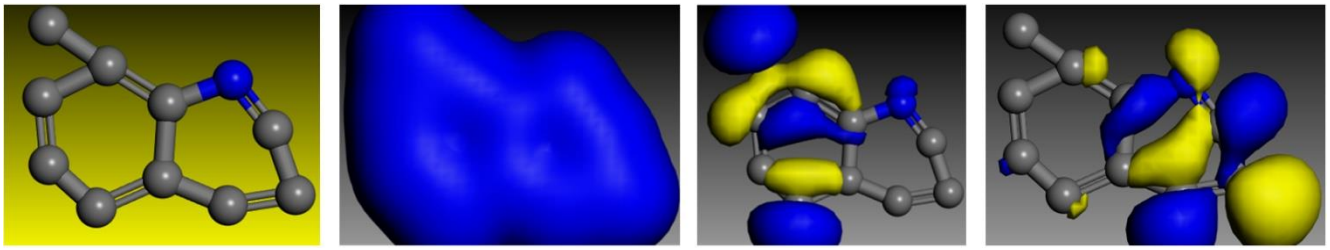

Figure 6. *Optimized structure, electrondensity, HOMO and LUMO of 8-MeQ.*

Table 1. *The Values of electronic parameters and Eigen values of 5-MeQ, 7-MeQ and 8-MeQ.*

Electronic/structural property	**5-MeQ**	**7-MeQ**	**8-MeQ**
HOMO (at orbital number)	68	68	68
LUMO (at orbital number)	69	69	69
E_{HOMO} (eV)	-4.969	-4.932	-4.886
E_{LUMO} (eV)	-3.092	-3.135	-3.141
ΔE (eV)	1.877	1.797	1.745
Molecular mass (g/mol) C_9H_9N	131	131	131
Ionization potential (*IP*) (eV)	4.969	4.932	4.886
Electron affinity (*EA*) (eV)	3.092	3.135	3.141
Absolute/Global hardness (η)	0.939	0.899	0.873
Global softness (σ)	1.065	1.112	1.146
Absolute electronegativity (χ)	4.031	4.034	4.014
Total number of electrons	67	67	67
Fraction of electrons transferred (ΔN)	0.835	0.871	0.909
Energy of back donation ($\Delta E_{b\text{-}d}$)	-0.235	-0.225	-0.218
Chemical Potential (μ) (eV)	-5.124	-6.012	-5.917
Electrophilicity Index (ω) (eV)	19.959	32.688	25.561
Nucleophilicity (ε) (eV)−1	0.035	0.038	0.039
Electron Accepting Power ($\omega+$) (eV)	21.519	28.522	26.328
Electron Donating Power ($\omega-$) (eV)	65.912	58.351	49.429
Net Electrophilicity ($\Delta\omega\pm$) (eV)	87.431	86.873	75.757

Quantum chemical calculations were performed in order to gain insights at the molecular level, electron distribution of the different inhibitor molecules used as well as to understand the nature of their interactions with the aluminium surfaces [17, 18]. The first consideration was to assess the electronic structures of the molecules, including the distribution of frontier molecular orbitals and Fukui indices, with a view to establish the active sites as well as local reactivity of the molecules [19]. In this research, 5, 7, and 8-methylquinolines are employed as the aluminium corrosion inhibitors tested theoretically in acid medium. The quantum chemical calculations for electronic and structural properties are shown in Table 1 of same substituent attached to the core quinoline. The most popular parameters which play a prominent role are the eigen values of the highest occupied molecular orbital (HOMO) and lowest unoccupied molecular orbital (LUMO), the HOMO-LUMO gap (ΔE), chemical hardness and softness, electro-negativity and the number of electrons transferred from inhibitor molecule to the metal surface [20, 21].

E_{HOMO}: Represents the energy of the highest occupied molecular orbital. It indicates the ability of a molecule to donate electrons (nucleophilicity). Higher E_{HOMO} values imply better electron-donating ability [22, 23]. According to the frontier molecular orbital theory (FMO) of chemical reactivity, transition of electron is due to an interaction between HOMO (highest occupied molecular orbital) and LUMO (lowest unoccupied molecular orbital) of reacting species [24]. The energy of HOMO is directly related to the ionization potential and characterizes the susceptibility of the molecule toward attack by electrophiles. Higher values of E_{HOMO} are likely to indicate a tendency of the molecule to donate electrons to appropriate acceptor molecules with low energy or empty electron orbital [25].

E_{LUMO} Represents the energy of the lowest unoccupied molecular orbital. Indicates the ability of a molecule to accept electrons (electrophilicity). Lower E_{LUMO} values imply better inhibition efficiency, as the molecule can accept electrons from the metal surface.

$$\Delta E = E_{LUMO} - E_{HOMO}$$

Represent energy gap. A smaller gap indicates easier electron transfer, facilitating corrosion inhibition. E_{HOMO}: Higher

values suggest better inhibition efficiency, as the molecule can donate electrons to the metal surface [26]. E_{LUMO}: Lower values indicate better inhibition efficiency, as the molecule can accept electrons from the metal surface [27]. Higher E_{HOMO} and lower E_{LUMO} values typically correspond to better corrosion inhibition efficiency [28]. A smaller ΔE (gap energy) indicates a more effective corrosion inhibiton. Among the three molecules used as aluminium corrosion inhibitors in this study, the molecule with higher E_{HOMO} and low E_{LUMO} is 5-MeQ. All the molecules used here inhibits the aluminium corrosion to high extent, but 5-MeQ here displays superior inhibition efficiency comparatively.

Global Hardness (η): Measures the resistance to electron density changes. Higher η indicates a harder molecule, less prone to polarization. The values of global hardness obtained here in Table 1 is relatively high for almost all the molecules but higher in 5-MeQ. This shows that the 5-MeQ molecule functions effectively without undergoing any polarization which may hinder performance. *Global Softness (σ)* is the inverse of global hardness. Higher σ indicates a softer molecule, more prone to polarization [29, 30].

Nucleophilicity: Measures the ability to donate electrons. Higher nucleophilicity indicates better electron-donating ability. The molecule 5-MeQ showed high nucleophilicity. This indicated direct confirmation of its better performance as inhibitor for aluminium corrosion [31].

Electrophilicity: Measures the ability to accept electrons. Higher electrophilicity indicates better electron-accepting ability [32]. 5-MeQ has the least electrophilicity among the three molecules. *Ionization Potential (IP)*: The energy required to remove an electron. Lower IP indicates easier electron removal. Table 1 shows that IP = 5-MeQ< 7-MeQ < 8-MeQ in order of increasing ionization potential comparatively.

Electron Affinity (EA): The energy released when an electron is added. Higher EA indicates easier electron addition [32]. Table 1 revealed that all the molecules used here have electron affinity, but 5-MeQ exhibits the highest.

Absolute Electronegativity (χ): A measure of the tendency to attract electrons. Higher χ indicates higher electronegativity. From the Table 1, 5-MeQ have highest values of (χ).

Chemical Potential (μ): Measures the tendency of a molecule to gain or lose electrons [33]. Lower μ indicates a higher tendency to gain. Generally the Table 1 shown the correlation between the chemical potential of each molecule and its aluminium corrosion inhibition performance.

Nucleophilicity Index (ε): A dimensionless parameter indicating nucleophilicity. Higher ω indicates better nucleophilicity [34]. There is a strong correlation between the value of ω and corrosion inhibition of each of the molecules as shown in Table 1 above. 5-MeQ exhibit higher ε comparably.

Electrophilicity Index (ω): A dimensionless parameter indicating electrophilicity. Higher ω indicates better electrophilicity [34]. The electrofilicity index of each of the above hydroxy-quinolines tested here as corrosion inhibitors for aluminium is approximately related to the performance of each molecule as indicated in Table 1 above.

Electron Accepting Power (ω^+): Measures the ability of a molecule to accept electrons. Higher ω^+ indicates better electron-accepting ability, enhancing corrosion inhibition. *Electron Donating Power (ω^-)*: Measures the ability of a molecule to donate electrons. Higher ω^- indicates better electron-donating ability, enhancing corrosion inhibition. The molecule 5-MeQ exhibit higher electron donating power (ω^+) as shown in the Table 1 above. *Net Electrophilicity ($\Delta\omega^{\pm}$)*: A comprehensive measure of electrophilicity, considering both electron-accepting and donating abilities. Higher $\Delta\omega^{\pm}$ indicates better overall electrophilicity, enhancing corrosion inhibition [35]. This is in agreement with what was obtained as shown in Table 1 for all the quinoline derivatives used here.

Energy of Back Donation (ΔE_{b-d}): Measures the energy associated with the back-donation of electrons from the metal surface to the inhibitor molecule. It indicates the strength of the feedback bond between the metal and inhibitor. Lower energy values indicate stronger back-donation, enhancing corrosion inhibition. It stabilizes the metal-inhibitor complex, reducing metal reactivity. There is low values of energy of back Donation for all the molecules as indicated in Table 1 above.

Fraction of Electron Transferred (ΔN): Measures the extent of electron transfer between the inhibitor and metal surface. It indicates the degree of charge transfer and covalent bonding. Higher ΔN values indicate more electron transfer, enhancing corrosion inhibition. ΔN facilitates the formation of a protective layer on the metal surface[35]. Generally there are adequate number of electrons transferred between the inhibitors and the metal for all the molecules used in this research. This has justified the inhibition performance of all the hydroxy quinoline molecules used as corrosion inhibitors for aluminium [35].

3.2. Quench Molecular Dynamic Simulation

Table 2. *The Statistical information for confirmation of electronic parameters for all the inhibitors.*

	5-Me	**7-MeQ**	**8-MeQ**
	K: H-(I+J)	**K: H-(I+J)**	**K: H-(I+J)**
Number of sample points	3	3	3

	5-Me **K: H-(I+J)**	**7-MeQ** **K: H-(I+J)**	**8-MeQ** **K: H-(I+J)**
Range	5.599100e-006	2.674590e-006	2.588430e-005
Maximum	-36.18401592	-37.69900337	-36.24262087
Minimum	-36.18402152	-37.69900604	-36.24264675
Mean	-36.18401828	-37.69900449	-36.24263015
Median	-36.18401742	-37.69900405	-36.24262283
Variance	5.599170e-012	1.287820e-012	1.384530e-010
Standard deviation	2.898060e-006	1.389870e-006	1.441110e-005
Mean absolute deviation	2.154730e-006	1.037270e-006	1.106790e-005
Skewness	-0.27190500	-0.28344900	-0.37688200
Kurtosis	-2.33333000	-2.33333000	-2.33333000

The statistical Table 2 provide insights into the electronic parameters of different quinoline derivatives based on the values of K:H−(I+J)K: H-(I+J)K:H−(I+J). Key statistical metrics such as range, mean, median, variance, standard deviation, skewness, and kurtosis have been used to describe the electronic behaviour of each molecule.

Variation in Electronic Parameters: The range of values varies significantly across the quinoline derivatives. *The 5-Me, 7-MeQ, and 8-MeQ* show extremely small ranges (in the order of 10−610^{-6}10−6 or lower), suggesting very stable electronic properties [36]. *The mean and median* values are very close for all the compounds, suggesting a symmetric distribution of data [36].

Skewness measures the asymmetry of the distribution.The 5-MeQ and 8-MeQ exhibit negative skewness, suggesting a longer left tail.Most values are close to zero, meaning the data is fairly symmetric [36].The *kurtosis* values are consistently around *-2.333*, suggesting a platykurtic distribution (flatter than a normal distribution).This means the data distributions are broad and have fewer extreme values (outliers) [37]. The Large variance and standard deviation indicate significant dispersion, meaning the electronic parameters fluctuate widely.Low variance (*8-MeQ: 1.38 × 10⁻¹⁶*) suggests very little variation, meaning highly stable electronic properties.The 5-Me, 7-MeQ, 8-MeQ compounds have very low range and variance, this has justified their stable electronic properties.This stability could make them more predictable for applications requiring consistent electronic behavior [37].

For Corrosion Inhibition: Stable electronic parameters may indicate consistent adsorption behavior, making these derivatives (5-Me, 7-MeQ and 8-MeQ) better corrosion inhibitors. *For Electronic Applications, 5-MeQ, 8-MeQ* could be useful in applications where consistent electronic properties are required due to their Low variance and high stability [38].

Table 3. *The Values of adsorption parameters for the interaction of 5-MeQ, 7-MeQ and 8-MeQ with the Al (110) surface.*

Adsorption properties(kcal/mol)	**5-MeQ**	**7-MeQ**	**8-MeQ**
Total kinetic energy	20.86564353	20.86564353	20.86564353
Total potential energy	49.33195320	28.73858242	43.85037143
Energy of molecule	57.03095656	64.92259834	80.09299230
Energy of Al(110) surface	0.00000000	0.00000000	0.00000000
Adsorption energy	-37.69900337	-36.18401592	-36.24262087

The binding energy (E_{bind}) between the metal surface and the inhibitor molecules are presented on Table 3. To quanti-

tatively estimate the interaction between each quinoline and the aluminium surface, the adsorption/binding energy, (E_{ads} / E_{bind}), was calculated using Equation: Binding Energy = E_{total} – ($E_{inhibitor}$ + $E_{Al\ surface}$). In each case, the potential energies were calculated by averaging the energies of each structure's lowest energy. As can be seen from the data, the binding (adsorption) energies are all negative suggesting stable adsorption structures [38]. However, the magnitude of the calculated binding energies is < 100 kcal mol^{-1}. This is despite the fact that the simulations did not take into consideration the specific covalent interactions between the molecules and the Al surface. This has been reported by by [38] to be in the range of physisorptive interactions. From the Table 3, it is observed that the binding energies for the quinoline molecules on Al (110) slab are of the magnitude between -30.60 to -50.69 (kcal mol^{-1}). This implies that the molecules are partly adsorbed on the Al surface. A detailed analysis of the on-top view of the adsorbed molecules on Al (110) emphasizing the soft epitaxial adsorption mechanism with accommodation of the molecular backbone in characteristic epitaxial grooves on the metal surface [38].

3.3. Fukui Indices

The sites at which an atom can bind to the metal surface is very important in corrosion studies. The figures in the prentices are the positions of each atom in the molecule, and the values outside are the extent of nuleophilic or electrophilic interaction of the atom with the aluminium surface as shown in Table 4 below.

Table 4. *Sites For Electrophilic And Nucleophilic Attack (Fukui Indices).*

	Electrophilic (F^-)				**Nucleophilic (F^+)**			
Molecule	**Mulliken**		**Hirshfeld**		**Mulliken**		**Hirshfeld**	
	Atom	**Value**	**Atom**	**Value**	**Atom**	**Value**	**Atom**	**Value**
5-MeQ	C (05)	0.105	C (03)	0.097	C (10)	0.120	C (10)	0.106
	C (09)	0.101	C (04)	0.091	C (04)	0.103	C (04)	0.102
	C (04)	0.092	C (07)	0.090	C (09)	0.102	C (05)	0.098
	C (10)	0.114	C (10)	0.102	C (05)	0.101	C (03)	0.097
	C (04)	0.106	C (07)	0.100	C (03)	0.099	C (09)	0.092
7-MeQ	C (05)	0.105	C (03)	0.097	C (10)	0.120	C (10)	0.106
	C (07)	0.101	C (04)	0.091	C (04)	0.103	C (04)	0.102
	C (04)	0.092	C (09)	0.090	C (09)	0.102	C (05)	0.098
	C (10)	0.114	C (10)	0.102	C (05)	0.101	C (03)	0.097
	C (04)	0.106	C (07)	0.100	C (03)	0.099	C (09)	0.092
8-MeQ	C (05)	0.105	C (03)	0.097	C (10)	0.120	C (10)	0.106
	C (08)	0.101	C (04)	0.091	C (04)	0.103	C (04)	0.102
	C (04)	0.092	C (09)	0.090	C (08)	0.102	C (05)	0.098
	C (10)	0.114	C (10)	0.102	C (05)	0.101	C (03)	0.097
	C (04)	0.106	C (04)	0.100	C (03)	0.099	C (08)	0.092

The Fukui functions derived from Density Functional Theory (DFT) calculations and provides insight into how electron density redistributes when adding or removing an electron [39]. The local reactivity of the inhibitor molecules was analyzed through the evaluation of Fukui indices. The condensed Fukui functions allowed us to distinguish each part of the molecule on the basis of its distinct chemical behaviour due to different functional group or substituent [40]. Thus, the site for nucleophilic attack will be the place where the value of F^+ is a maximum and the site for electrophilic attack will be the place where the value of F^- is maximum [40].

The values of the Fukui functions for a nucleophilic and electrophilic attack for all the inhibitors as given in Table 4 (for the nitrogen the carbon atoms). Inspection of the values of

Fukui functions presented shows that the quinoline derivatives have propitious zones for nucleophilic cattack located on (C and N). The HOMO location on each molecule agrees with the atoms that exhibit greatest values of indices of Fukui, both indicated the zones by which the molecule would be adsorbed on the aluminium surface [40].

Electrophilic Attack Susceptibility: This measures the change in electron density when an electron is added to the system.High values electrophilic attack susceptibility indicate regions that are more susceptible to electrophilic attack.In quinoline derivatives, this is crucial for understanding interactions with electrophilic species, such as protons or metal ions[40].

Nucleophilic Attack Susceptibility: This measures the change in electron density when an electron is removed from the system.High values of nucleophilic attack susceptibility indicate sites where nucleophiles are likely to attack.This is particularly useful in studying quinoline derivatives' interactions in redox reactions [41].

For the*5-MeQ, 7-MeQ, and 8-MeQ*, the presence of the methyl (-Me) group slightly modifies the electron density distribution, affecting reactivity.Typically, methyl groups donate electron density, making adjacent positions more susceptible to electrophilic attack.

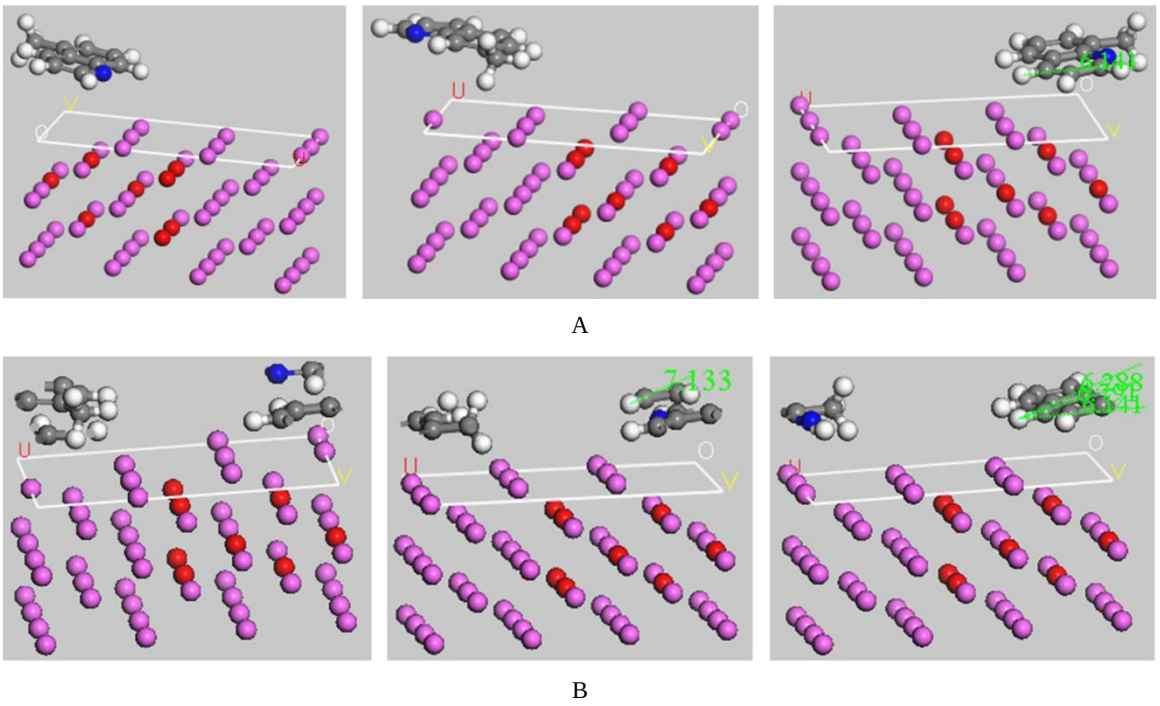

Figure 7. *The final side snapshots of adsorbed 5-MeQ, 7-MeQ and 8-MeQ molecules, from left to right respectively, on aluminium (110) reflection. (A) Single molecules. (B) Many molecule.*

Further information on the interaction between the inhibitors and the aluminium surface can be provided by the molecular dynamics simulations. The adsorption of quinoline derivatives molecules on the aluminium surfaces were analyzed at a molecular level by molecular dynamics simulations, using Forcite quench molecular dynamics to sample many different low energy configurations and to identify the low energy minima [42]. As shown in Figure 7, the optimized molecules were used for the simulation. Solvent and charge effects were neglected in all the simulations and calculations were performed at the metal/vacuum interface [42]. Although this is clearly an over simplification of the actual situation, it is adequate to qualitatively illustrate the differences in the adsorption behaviour of the molecules and provide sufficient insight to the study objectives [43].

Figure7 shows representative snapshots of the cross-section of the lowest energy adsorption configurations for the single molecules on the Al (110) surface from the top (A) and for more than one molecule from the bottom (B). The molecules can be seen to maintain a flat-lying adsorption orientation on the metal surface thereby maximizing contact and enhancing the degree of surface coverage. This parallel adsorption orientation also facilitates interaction of π - electrons of the quinoline nucleus and the heteroatom (N) in the molecules with the metal surfaces [44].

4. Conclusion

From the analysis of the quantum chemical parameters, the adsorption parameters from the simulation of the molecules, the Mulliken and Hirshfeld values of the fukui indices for the three molecules of methylquinolines (5-MeQ, 7-MeQ and 8-MeQ); all the three molecules exhibits very high potential

for inhibition of aluminium corrosion in HCl environment. However, 5-MeQ is superior to 7-MeQ and 8-MeQ. The difference in the quantum chemical properties responsible for high inhibition efficiency shown by the molecules despite having the same mass and structure is believed to come from orientation of the methly substituent ($-CH_3$) position on the parent quinoline molecule. Intra-molecular interaction is suspected to occurred in 7-MeQ and 8-MeQ which leads to poor donation of free electron from the entire molecule in the formation of the metal-inhibitor complex. The stronger the intra-molecular interaction, the slower the complex formation hence reduced inhibition efficiency. Methyl group at position 5 do not likely form intra-molecular interaction, as a result, 5-MeQ readily form complex with the aluminium and displayed excellent properties for higher corrosion inhibition performance than other two molecules. Corrosion inhibition efficiency of heterocyclic compound can be influence by the position of substituent attached to the parent molecule.

Abbreviations

5-MeQ	5-Methylquinoline
5-MeQ	7-Methylquinoline
5-MeQ	8-Methylquinoline
DFT	Density Functional Theory
MD	Molecular Dynamic
HOMO	Highest Occupied Molecular Orbital
LUMO	Lowest Unoccupied Molecular Orbital
E_{HOMO}	Energy of Highest Occupied Molecular Orbital
E_{LUMO}	Energy of Lowest Unoccupied Molecular Orbital

Author Contributions

Abdulmumin Malam Usman: Conceptualization, Funding acquisition, Writing – original draft

Ayuba Abdullahi Muhammad: Project administration, Supervision

Jaweria Ambreen: Project administration, Supervision

Conflicts of Interest

The authors declared no conflicts of interest.

References

[1] Abdel-Gaber, A. M., Khamis, E., Abo-El Dahab, M., & Abd-El-Khalek, N. A. (2009). Schiff bases as corrosion inhibitors for aluminum in H_2SO_4 solution. Corrosion Science, 51(5), 1038-1045.

[2] Abdul Rahiman, A. K., & Sethumanickam, S. (2014). Inhibition of mild steel corrosion using Juniperus plants as green inhibitor. *African Journal of Pure and Applied Chemistry*, 8(1), 9-22.

[3] Abdul Rahiman, M., & Sethumanickam, A. (2014). Corrosion inhibition of aluminium using organic inhibitors in acidic medium. International Journal of Research in Chemical Science, 4(3), 22-30.

[4] Abeng, F. E., Anadebe, V., Nkom, P. Y., Uwakwe, K. J., & Kamalu, E. G. (2022). Experimental and theoretical study on the corrosion inhibitor potential of quinazoline derivative for mild steel in hydrochloric acid solution. Journal of Electrochemical Science and Engineering, 12(3), 243–257.

[5] Beltrán-Prieto, C., Serrano, A. A. A., Solís-Rodríguez, G., Martínez, A., Orozco-Cruz, R., Espinoza-Vázquez, A., & Miralrio, A. (2022). A General Use QSAR-ARX Model to Predict the Corrosion Inhibition Efficiency of Commercial Drugs on Steel Surfaces. *International Journal of Molecular Sciences*, 23(9), 5086.

[6] Bostan, R., & Popa, A. (2012). Evaluation of some phenothiazine derivatives as corrosion inhibitors for bronze in weakly acidic solution. Journal of Applied Electrochemistry, 42(4), 321-328.

[7] Brycki, B., Szulc, A., Kowalczyk, I., & Koziróg, A. (2017).Organic corrosion inhibitors. International Journal of Corrosion and Scale Inhibition, 6(4), 354-372.

[8] Callister, W. D., Jr. (2001).Materials Science and Engineering: An Introduction (6th ed).

[9] Cao, C. (1996).Study on the relationship between the corrosion interface structure and negative difference effect for pure magnesium. Corrosion Science and Protection Technology, 8(3), 205-210.

[10] Chahul, H. F., Gbertyo, T. S., & Iorungwa, M. S. (2015). Adsorption and corrosion inhibition properties of Cissus populnea stem extract on aluminium in hydrochloric acid solutions. Journal of Materials and Environmental Science, 6(5), 1443-1452.

[11] Chavan N. D., V. Vijayakumar (2024). Synthesis, DFT Studies on a Series of Tunable Quinoline Derivatives. RSC Advances 14 (21089-21101), https://doi.org/10.1039/D4RA03961K

[12] Chi, M. and Zhao, Y.P. (2009). Adsorption of formaldehyde molecule on the intrinsic and Al-doped grapheme: A first principle study. Computional Materials Science, 48: 1085-1090.

[13] Chi, Y., & Zhao, Y. (2009).Chi phase after short-term aging and corrosion behavior in 2205 duplex stainless steel. Journal of Iron and Steel Research International, 16(6), 65-70.

[14] Ebenso, E. E., Eddy, N. O., & Odiongenyi, A. O. (2008).Corrosion inhibitive properties and adsorption behavior of ethanol extract of Piper guinensis as a green corrosion inhibitor for mild steel in H_2SO_4. African Journal of Pure and Applied Chemistry, 2(11), 107-115.

[15] Ebenso, E. E., et al. (2010).Corrosion inhibition and adsorption properties of ethanol extract of Gongronema latifolium on mild steel in H_2SO_4. Portugaliae Electrochimica Acta, 28(1), 13-22.

[16] Fu, J., Li, S., & Wang, Y. (2020).Computational and electrochemical studies of some amino acid compounds as corrosion inhibitors for mild steel in hydrochloric acid solution. Journal of Molecular Liquids, 309, 113102.

[17] Fu, J., Zhang, H., Wang, Y., Li, S., Chen, T., & Liu, X. (2012). Experimental and Theoretical Study on the Inhibition Performances of Quinoxaline and Its Derivatives for the Corrosion of Mild Steel in Hydrochloric Acid. *Industrial & Engineering Chemistry Research*, 51(16), 6377-6386.

[18] Gece, G., & Bilgiç, S. (2010).A theoretical study on the inhibition efficiencies of some amino acids as corrosion inhibitors of nickel. Corrosion Science, 52(10), 3435-3443.

[19] Giovanny Carvalho dos Santos, Roberta Oliveira Servilha, Eliézer Fernando de Oliveira, Francisco Carlos Lavarda, Valdecir Farias Ximenes, Luiz Carlos da Silva-Filho (2017). Theoretical-Experimental Photophysical Investigations of the Solvent Effect on the Properties of Green- and Blue-Light-Emitting Quinoline Derivatives, *Journal of Fluorescence*, 27(2) 709-1720. https://doi.org/10.1007/s10895-017-2108-0

[20] Goyal, M., Kumar, S., Bahadur, I., Verma, C., & Ebenso, E. E. (2018).Organic corrosion inhibitors for industrial cleaning of ferrous and non-ferrous metals in acidic solutions: A review. Journal of Molecular Liquids, 256, 565-573.

[21] Hussin, M. H., & Kassim, M. J. (2010). The corrosion inhibition of mild steel by plant extract in acidic medium. Journal of Corrosion Science and Engineering, 12(1), 45-52.

[22] Ibrahim, J., et al. (2021).Corrosion inhibition potential of ethanol extract of Acacia nilotica leaves on mild steel in an acidic medium. Journal of Materials and Environmental Science, 12(1), 1-10.

[23] Jakub Wantulok, Marcin Szala, Andrea Quinto, Jacek E. Nycz, Stefania Giannarelli, Romana Sokolová, Maria Książek and Joachim Kusz (2020). Synthesis, Electrochemical and Spectroscopic Characterization of Selected Quinolinecarbaldehydes and Their Schiff Base Derivatives. *Journal:* Molecules 25(9) 2053. https://doi.org/10.3390/molecules25092053

[24] Kadapparambil Sumithra, Kavita Yadav, Manivannan Ramachandran and Noyel Victoria Selvam (2017b). Electrochemical investigation of the corrosion inhibition mechanism of *Tectona grandis* leaf extract for SS304 stainless steel in hydrochloric acid, *De Gruyter*,https://doi.org/10.1515/corrrev-2016-0074

[25] Khaled, K. F., Sherif, E. M., & Hamed, F. (2016). Effect of cerium chloride on corrosion inhibition of aluminum in seawater. Journal of Applied Electrochemistry, 46(3), 187-197.

[26] Kiani M. A. Mousavi, M. F., Ghasemi, S. Shamsipur, M. and Kazemi, S. H. (2008). Inhibitory effect of some amino acids on corrosion of Pb-Ca-Sn alloy in sulphuric acid solution.*Corrosion Science* 50: 1035-1045.

[27] Nnanna, L. A., Uroh, C. A., & Mejeha, I. M. (2016). Corrosion inhibition efficiency of Pentaclethra macrophylla root extract on mild steel in alkaline medium. ResearchJournal of Chemical Sciences, 6(1), 42-50.

[28] Nosonovsky, M. (2015).Coupling of surface energy with electric potential makes superhydrophobic surfaces corrosion-resistant. Physical Chemistry Chemical Physics, 17(35), 22830-22835.

[29] Obot, I. B., & Eduok, U. M. (2017).The use of green corrosion inhibitors: A review. Green Chemistry Letters and Reviews, 10(3), 223-241.

[30] Olufunmilayo, A. O., Olusegun, K. M., & Olusegun, J. K. (2020). Fourier Transform Infrared Spectroscopy Applications: Exploiting the Potentials for Analytical Purposes. Journal of Natural Sciences Research, 10(3), 1-14. https://doi.org/10.7176/JNSR/10-3-01

[31] Patni, N., Agarwal, S., & Shah, P. (2013). Green corrosion inhibitors: A sustainable approach. Corrosion Science, 53(6), 4023-4037.

[32] Pavithra, M. K., Venkatesha, T. V., & Vathsala, K. (2012). Inhibition of mild steel corrosion in acid media by Rabeprazole sulfide. *Journal of Corrosion Science*, 60, 104-111.

[33] Qiang Y., S. Zhang, B. Tan, and S. Chen (2018), "Evaluation of Ginkgo leaf extract as an eco-friendly corrosion inhibitor of X70 steel in HCl solution," *Corrosion Science*, 13(3), 6-18.

[34] Rajendran, S., Anthony, N., Ramaraj, R., & Jayasree, P. (2008). Corrosion inhibition by Phyllanthus amarus, Allium sativum, rhizome powder, and beet root extract. Bulletin of Electrochemistry, 24(9), 105-112.

[35] Saedah, H. A. (2014). Corrosion inhibition of aluminium in hydrochloric acid by Allium sativum (Garlic) extract. International Journal of Electrochemical Science, 9(12), 7643-7652.

[36] Talari, A. C. S., Martinez, M. A. M., Movasaghi, Z., Rehman, S., & Rehman, I. U. (2017). Advances in Fourier transform infrared (FTIR) spectroscopy of biological tissues. Applied Spectroscopy Reviews, 52(5), 456-506. https://doi.org/10.1080/05704928.2016.1230863

[37] Talbot D. E. J., and J. D. R. Talbot (2018). Corrosion Science and Technology, 3rd ed. New York: Taylor and Francis, pp. 159-194.

[38] Umoren, S. A., Obot, I. B., & Ebenso, E. E. (2009). Gum arabic as a potential corrosion inhibitor for aluminium in acidic medium. Pigment & Resin Technology, 38(1), 33-40.

[39] Verma C., Olasunkanmi L.O. and Ebenso E.E. (2016a). Adsorption behavior of glucosamine-based, pyrimidine-fused heterocycles as green corrosion inhibitors for mild steel: experimental and theoretical studies. *Journal Phys Chem.;*Vol. 120(21): 11598. https://doi.org/10.1021/acs.jpcc.6b04429

[40] Wahyuningrum, D., et al. (2008).The correlation between structure and corrosion inhibition activity of 4, 5-diphenyl-1-vinylimidazole derivative compounds towards mild steel in 1 N NaCl solution. Journal of Applied Sciences, 8(23), 4463-4469.

[41] Xhanari, K., & Finšgar, M. (2016). Organic corrosion inhibitors for aluminium and its alloys in acid solutions: A review. RSC Advances, 6(67), 62833-62870.

[42] Xiong, S., Sun, J. L., Xu, Y., & Yan, X. D. (2016). QSAR Study on Imidazole Derivatives as Corrosion Inhibitors by Genetic Function Approximation Method. *Materials Science Forum*, 850, 426-432.

[43] Yuhong, Z., Jingli, Y., & Haibo, Y. (2011). Computational and experimental studies on the corrosion inhibition of mild steel in acid media using organic inhibitors. Journal of Molecular Structure, 987(3), 74-81.

[44] Zhang H., Y. Chen, Z. Zhang, (2018). Comparative studies of two benzaldehydethiosemicarbazone derivatives as corrosion in- hibitors for mild steel in 1.0 M HCl, Result Phys. 11) 554e563, https://doi.org/10.1016/j.rinp.09.038